

Large Momentum Transfer Measurements of the Deuteron Elastic Structure Function $A(Q^2)$ at Jefferson Laboratory

L.C. Alexa,²⁵ B.D. Anderson,¹⁴ K.A. Aniol,² K. Arundell,³⁴ L. Auerbach,³⁰ F.T. Baker,⁷ J. Berthot,¹ P.Y. Bertin,¹ W. Bertozzi,¹⁸ L. Bimbot,²³ W.U. Boeglin,⁴ E.J. Brash,²⁵ V. Breton,¹ H. Breuer,¹⁷ E. Burtin,²⁷ J.R. Calarco,¹⁹ L.S. Cardman,³¹ C. Cavata,²⁷ C.-C. Chang,¹⁷ J.-P. Chen,³¹ E. Chudakov,³¹ E. Cisbani,¹³ D.S. Dale,¹⁵ N. Degrande,⁶ R. De Leo,¹¹ A. Deur,¹ N. d'Hose,²⁷ B. Diederich,²² J.J. Domingo,³¹ M.B. Epstein,² L.A. Ewell,¹⁷ J.M. Finn,³⁴ K.G. Fissum,¹⁸ H. Fonvieille,¹ B. Frois,²⁷ S. Frullani,¹³ H. Gao,¹⁸ J. Gao,¹⁸ F. Garibaldi,¹³ A. Gasparian,^{9,15} S. Gilad,¹⁸ R. Gilman,²⁶ A. Glamazdin,¹⁶ C. Glashauser,²⁶ J. Gomez,³¹ V. Gorbenko,¹⁶ J.-O. Hansen,³¹ R. Holmes,²⁹ M. Holtrop,¹⁹ C. Howell,³ G.M. Huber,²⁵ C. Hyde-Wright,²² M. Iodice,¹³ C.W. de Jager,³¹ S. Jaminion,¹ J. Jardillier,²⁷ M.K. Jones,³⁴ C. Jutier,^{1,22} W. Kahl,²⁹ S. Kato,³⁵ A.T. Katramatou,¹⁴ J.J. Kelly,¹⁷ S. Kerhoas,²⁷ A. Ketikyan,³⁶ M. Khayat,¹⁴ K. Kino,³² L.H. Kramer,⁴ K.S. Kumar,²⁴ G. Kumbartzki,²⁶ M. Kuss,³¹ G. Lavessière,¹ A. Leone,¹² J.J. LeRose,³¹ M. Liang,³¹ R.A. Lindgren,³³ N. Liyanage,¹⁸ G.J. Lolos,²⁵ R.W. Lourie,²⁸ R. Madey,^{9,14} K. Maeda,³² S. Malov,²⁶ D.M. Manley,¹⁴ D.J. Margaziotis,² P. Markowitz,⁴ J. Marroncle,²⁷ J. Martino,²⁷ C.J. Martoff,³⁰ K. McCormick,²² J. McIntyre,²⁶ R.L.J. van der Meer,²⁵ S. Mehrabyan,³⁶ Z.-E. Meziani,³⁰ R. Michaels,³¹ G.W. Miller,²⁴ J.Y. Mougey,⁸ S.K. Nanda,³¹ D. Neyret,²⁷ E.A.J.M. Offermann,³¹ Z. Papandreou,²⁵ C.F. Perdrisat,³⁴ R. Perrino,¹² G.G. Petratos,¹⁴ S. Platchkov,²⁷ R. Pomatsalyuk,¹⁶ D.L. Prout,¹⁴ V.A. Punjabi,²⁰ T. Pussieux,²⁷ G. Quémenér,³⁴ R.D. Ransome,²⁶ O. Ravel,¹ Y. Roblin,¹ D. Rowntree,¹⁸ G. Rutledge,³⁴ P.M. Rutt,²⁶ A. Saha,³¹ T. Saito,³² A.J. Sarty,⁵ A. Serdarevic,^{25,31} T. Smith,¹⁹ K. Soldi,²¹ P. Sorokin,¹⁶ P.A. Souder,²⁹ R. Suleiman,¹⁴ J.A. Templon,⁷ T. Terasawa,³² L. Todor,²² H. Tsubota,³² H. Ueno,³⁵ P.E. Ulmer,²² G.M. Urciuoli,¹³ L. Van Hoorebeke,⁶ P. Vernin,²⁷ B. Vlahovic,²¹ H. Voskanyan,³⁶ J.W. Watson,¹⁴ L.B. Weinstein,²² K. Wijesooriya,³⁴ R. Wilson,¹⁰ B.B. Wojtsekhowski,³¹ D.G. Zainea,²⁵ W.-M. Zhang,¹⁴ J. Zhao,¹⁸ and Z.-L. Zhou.¹⁸

(The Jefferson Lab Hall A Collaboration)

¹Université Blaise Pascal/IN2P3, F-63177 Aubière, France. ²California State University at Los Angeles, Los Angeles, CA 90032. ³Duke University, Durham, NC 27706. ⁴Florida International University, Miami, FL 33199. ⁵Florida State University, Tallahassee, FL 32306. ⁶University of Gent, B-9000 Gent, Belgium. ⁷University of Georgia, Athens, GA 30602. ⁸Institut des Sciences Nucléaires, F-38026 Grenoble, France. ⁹Hampton University, Hampton, VA 23668. ¹⁰Harvard University, Cambridge, MA 02138. ¹¹INFN, Sezione di Bari and University of Bari, 70126 Bari, Italy. ¹²INFN, Sezione di Lecce, 73100 Lecce, Italy. ¹³INFN, Sezione Sanità and Istituto Superiore di Sanità, 00161 Rome, Italy. ¹⁴Kent State University, Kent OH 44242. ¹⁵University of Kentucky, Lexington, KY 40506. ¹⁶Kharkov Institute of Physics and Technology, Kharkov 310108, Ukraine. ¹⁷University of Maryland, College Park, MD 20742. ¹⁸Massachusetts Institute of Technology, Cambridge, MA 02139. ¹⁹University of New Hampshire, Durham, NH 03824. ²⁰Norfolk State University, Norfolk, VA 23504. ²¹North Carolina Central University, Durham, NC 27707. ²²Old Dominion University, Norfolk, VA 23508. ²³Institut de Physique Nucléaire, F-91406 Orsay, France. ²⁴Princeton University, Princeton, NJ 08544. ²⁵University of Regina, Regina, SK S4S 0A2, Canada. ²⁶Rutgers, The State University of New Jersey, Piscataway, NJ 08855. ²⁷CEA Saclay, F-91191 Gif-sur-Yvette, France. ²⁸State University of New York at Stony Brook, Stony Brook, NY 11794. ²⁹Syracuse University, Syracuse, NY 13244. ³⁰Temple University, Philadelphia, PA 19122. ³¹Thomas Jefferson National Accelerator Facility, Newport News, VA 23606. ³²Tohoku University, Sendai 980, Japan. ³³University of Virginia, Charlottesville, VA 22901. ³⁴College of William and Mary, Williamsburg, VA 23187. ³⁵Yamagata University, Yamagata 990, Japan. ³⁶Yerevan Physics Institute, Yerevan 375036, Armenia.

Submitted to Physical Review Letters
(October 28, 1998)

The deuteron elastic structure function $A(Q^2)$ has been extracted in the range $0.7 \leq Q^2 \leq 6.0$ $(\text{GeV}/c)^2$ from cross section measurements of elastic electron-deuteron scattering in coincidence using the Hall A Facility of Jefferson Laboratory. The data are compared to theoretical models based on the impulse approximation with the inclusion of meson-exchange currents, and to predictions of quark dimensional scaling and perturbative quantum chromodynamics.

Electron scattering from the deuteron has long been a crucial tool in understanding the internal structure and dynamics of the nuclear two-body system. In particular, the deuteron electromagnetic form factors, measured in elastic scattering, offer unique opportunities to test models of the short-range nucleon-nucleon interaction, meson-exchange currents and isobaric configurations as well as the possible influence of explicit quark degrees of freedom [1], [2].

The cross section for elastic electron-deuteron (e-d) scattering is described by the Rosenbluth formula:

$$\frac{d\sigma}{d\Omega} = \sigma_M \left[A(Q^2) + B(Q^2) \tan^2\left(\frac{\theta}{2}\right) \right] \quad (1)$$

where $\sigma_M = \alpha^2 E' \cos^2(\theta/2) / [4E^3 \sin^4(\theta/2)]$ is the Mott cross section. Here E and E' are the incident and scattered electron energies, θ is the electron scattering angle, $Q^2 = 4EE' \sin^2(\theta/2)$ is the four-momentum transfer squared and α is the fine structure constant. The elastic electric and magnetic structure functions $A(Q^2)$ and $B(Q^2)$ are given in terms of the charge, quadrupole and magnetic form factors $F_C(Q^2)$, $F_Q(Q^2)$, $F_M(Q^2)$:

$$A(Q^2) = F_C^2(Q^2) + \frac{8}{9}\tau^2 F_Q^2(Q^2) + \frac{2}{3}\tau F_M^2(Q^2) \quad (2)$$

$$B(Q^2) = \frac{4}{3}\tau(1 + \tau)F_M^2(Q^2) \quad (3)$$

where $\tau = Q^2/4M_d^2$, with M_d being the deuteron mass.

The interaction between the electron and the deuteron is mediated by the exchange of a virtual photon. In the non-relativistic impulse approximation (IA), where the photon is assumed to interact with one of the two nucleons in the deuteron, the deuteron form factors are described in terms of the deuteron wave function and the electromagnetic form factors of the nucleons. Theoretical calculations based on the IA approach [1] using various nucleon-nucleon potentials and parametrizations of the nucleon form factors generally underestimate the existing $A(Q^2)$ data [3], [4], [5], [6]. Recent relativistic impulse approximation (RIA) calculations improve or worsen the agreement with the data depending on their particular assumptions. There are two RIA approaches: manifestly covariant calculations [7], [8] and light-front dynamics [9], [10].

It is well known that the form factors of the deuteron are very sensitive to the presence of meson-exchange currents (MEC) [1]. There have been numerous extensive studies and calculations augmenting both the IA and RIA approaches with the inclusion of MEC. The principal uncertainties in these calculations are the poorly known value of the $\rho\pi\gamma$ coupling constant and the $\rho\pi\gamma$ vertex form factor. Some calculations show also sensitivity to possible presence of isobar configurations in the deuteron [11]. The inclusion of MEC brings the theory into better agreement with the existing data.

It is widely recognized that the underlying quark-gluon dynamics cannot be ignored at distances much less than the nucleon size. This has led to the formulation of so-called hybrid quark models [12] that try to simultaneously incorporate the quark- and gluon-exchange mechanism at short distances and the meson-exchange mechanism at long and intermediate distances. When the inter-nucleon separation is smaller than ~ 1 fm, the deuteron is treated as a six-quark configuration with a certain probability that results in an additional contribution to the deuteron form factors.

At sufficiently large momentum transfers the form factors are expected to be calculable in terms of only quarks and gluons within the framework of quantum chromodynamics (QCD). The first attempt at a quark-gluon description of the deuteron form factors was based on quark-dimensional scaling (QDS) [13]. The underlying dynamical mechanism during e-d scattering is the rescattering of the constituent quarks via the exchange of hard gluons. The Q^2 dependence of this process is then predicted by simply counting the number of gluon propagators (5), which implies that $\sqrt{A(Q^2)} \sim (Q^2)^{-5}$. This prediction was later substantiated in the framework of perturbative QCD (pQCD), where it was shown [14] that in leading-order: $\sqrt{A(Q^2)} = [\alpha_s(Q^2)/Q^2]^5 \sum_{m,n} d_{mn} [\ln(Q^2/\Lambda^2)]^{-\gamma_n - \gamma_m}$ where $\alpha_s(Q^2)$ and Λ are the QCD strong coupling constant and scale parameter, and $\gamma_{m,n}$ and d_{mn} are QCD anomalous dimensions and constants. The existing SLAC $A(Q^2)$ data [4] exhibit some evidence of this asymptotic fall-off for $Q^2 > 2$ (GeV/c)².

The unique features of the Continuous Electron Beam Accelerator and Hall A Facilities of the Jefferson Laboratory (JLab) offered the opportunity to extend the kinematical range of $A(Q^2)$ and to resolve inconsistencies in previous data sets from different laboratories by measuring the elastic e-d cross section for $0.7 \leq Q^2 \leq 6.0$ (GeV/c)². Electron beams of 100% duty factor were scattered off a liquid deuterium target in Hall A. Scattered electrons were detected in the electron High Resolution Spectrometer (HRSE). To suppress backgrounds and separate elastic from inelastic processes, recoil deuterons were detected in coincidence with the scattered electrons in the hadron HRS (HRSH). Elastic electron-proton (e-p) scattering in coincidence was used to calibrate this double-arm system. A schematic of the Hall A Facility as used in this experiment is shown in Figure 1.

The incident beam energy was varied between 3.2 and 4.4 GeV. The beam intensity, 5 to 120 μ A, was monitored using two resonant cavity beam current monitors (BCM) upstream of the target system. The two cavities were frequently calibrated against a parametric current transformer monitor (Unser monitor) [15]. The beam was rastered on the target in both horizontal and vertical directions at high frequency and its position was monitored

with two beam position monitors (BPM). The uncertainties in the incident beam current and energy were estimated to be $\pm 2\%$ and $\pm 0.2\%$, respectively.

The target system contained liquid hydrogen and deuterium cells of length $T=15$ cm. Two Al foils separated by 15 cm were used to measure the contribution to the cross section from the Al end-caps of the target cells. The liquid hydrogen(deuterium) was pressurized to 1.8(1.5) atm and pumped at high velocity (~ 0.5 m/s) through the cells to heat exchangers. The hydrogen(deuterium) temperature was 19(22) K. This system provided a record high luminosity of $4.0 \times 10^{38} \text{cm}^{-2} \text{s}^{-1}$ ($4.7 \times 10^{38} \text{cm}^{-2} \text{s}^{-1}$) for hydrogen(deuterium). The raster system kept beam-induced density changes at a tolerable level: up to 2.5%(5.0%) at $120 \mu\text{A}$ for deuterium(hydrogen).

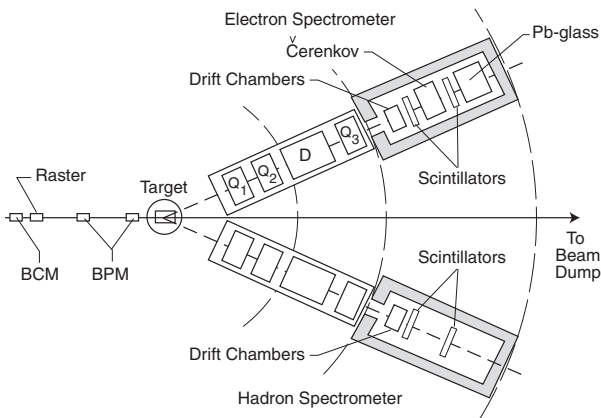


FIG. 1. Plan view of the Hall A Facility of JLab as used in this experiment. Shown are the beam monitoring devices, the cryo-target, the two magnetically identical spectrometers (consisting of quadrupoles Q_1 , Q_2 , Q_3 , and dipole D), and the detector packages.

Scattered electrons were detected in HRSE used in its standard configuration consisting of two planes of plastic scintillators to form an “electron” trigger, a pair of drift chambers for electron track reconstruction, and a gas threshold Čerenkov counter and a segmented lead-glass calorimeter for electron identification. Recoil nuclei were detected in HRSH using a subset of its detection system: two planes of scintillators to form a “recoil” trigger and a pair of drift chambers for recoil track reconstruction. The efficiencies of the calorimeter and Čerenkov counter were $\sim 99.5\%$, and of scintillators and tracking almost 100% for both spectrometers. Event triggers consisted of electron-recoil coincidences and of a prescaled sample of electron and recoil single-arm triggers.

Electron events were identified on the basis of a minimal pulse height in the Čerenkov counter and an energy deposited in the calorimeter consistent with the momentum determined from the drift chamber track. Coincidence events were identified using the relative time-of-flight (TOF) between the electron and recoil triggers.

Contributions from the target cell end-caps and random coincidences were negligible. Elastic e-p scattering was measured for each e-d elastic kinematics. The e-p kinematics was chosen to match the electron-recoil solid angle Jacobian for the corresponding e-d kinematics. Data were taken with and without acceptance defining collimators in front of the spectrometers.

The elastic e-p and e-d cross sections were calculated using:

$$\frac{d\sigma}{d\Omega} = \frac{N_{ep(d)} C_{eff}}{N_i N_t (\Delta\Omega)_{MC} F} \quad (4)$$

where $N_{ep(d)}$ is the number of e-p(e-d) elastic events, N_i is the number of incident electrons, N_t is the number of target nuclei/cm², $(\Delta\Omega)_{MC}$ is the effective double-arm acceptance from a Monte Carlo simulation, F is the portion of radiative corrections that depends only on Q^2 and T (1.088 and 1.092, on average, for e-p and e-d elastic respectively) and $C_{eff} = C_{det} C_{cdt} C_{rni}$. Here C_{det} is the electron and recoil detector and trigger inefficiency correction (2.6%), C_{cdt} is the computer dead-time correction (typically 10% for e-d elastic), and C_{rni} is the correction for losses of recoil nuclei due to nuclear interactions in the target (0.7-1.8% for protons and 2.8-5.1% for deuterons).

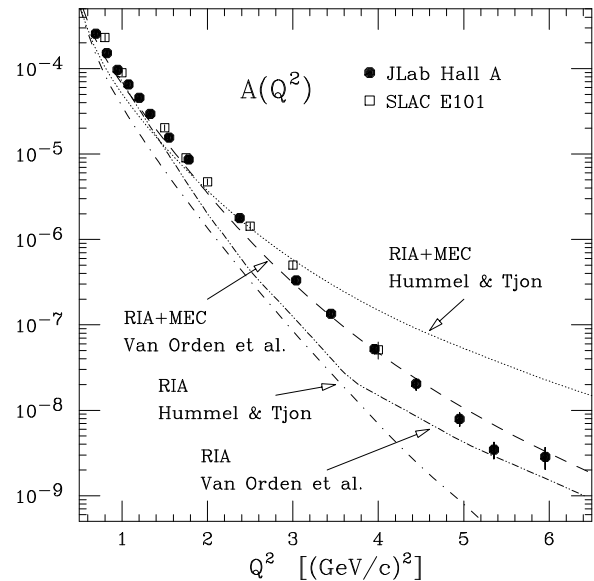


FIG. 2. The deuteron elastic structure function $A(Q^2)$ from this experiment compared to RIA theoretical calculations [7], [8]. Also shown are previous SLAC data [4].

The effective double-arm acceptance was evaluated with a Monte Carlo computer program that simulated elastic e-p and e-d scattering under identical conditions as our measurements. The program tracked scattered electrons and recoil nuclei from the target to the detectors through the two HRS’s using optical models based on magnetic measurements of the quadrupole and dipole elements and on position surveys of collimation systems,

magnets and vacuum apertures. The effects from ionization energy losses and multiple scattering in the target and vacuum windows were taken into account for both electrons and recoil nuclei. Bremsstrahlung radiation losses for both incident and scattered electrons in the target and vacuum windows as well as internal radiative effects were also taken into account. Details on this simulation method can be found in Ref. [18]. Monte Carlo simulated spectra of scattered electrons and recoil nuclei were found to be in very good agreement with experimentally measured spectra.

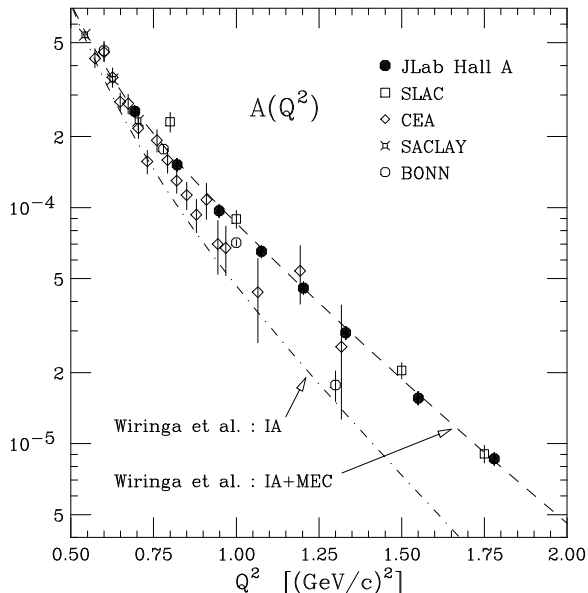


FIG. 3. The present $A(Q^2)$ data compared with overlapping data from CEA [3], SLAC [4], Bonn [5], Saclay [6], and IA+MEC theoretical calculations [25].

The e-p elastic cross sections measured with the acceptance defining collimators were found to agree within 0.3%, on average, with values calculated using a recent fit [17] to world data of the proton form factors. The e-p elastic cross sections measured without the collimators were, on average, 2.6% higher than the ones measured with collimators. All e-d cross section data taken without collimators have been normalized by 2.6%.

Values for $A(Q^2)$ were extracted from the measured e-d cross sections under the assumption that $B(Q^2)$ does not contribute to the cross section (supported by the existing $B(Q^2)$ data [16]). The extracted $A(Q^2)$ values are presented in Fig. 2 together with previous SLAC data [4] and theoretical calculations. The error bars represent statistical and systematic uncertainties added in quadrature. The statistical error ranged from $\pm 1\%$ to $\pm 28\%$. The systematic error has been estimated to be $\pm 5.9\%$ and is dominated by the uncertainty in $(\Delta\Omega)_{MC}$ ($\pm 3.6\%$). Each of the two highest Q^2 points represents the average of two measurements with different beam energies (4.0 and 4.4 GeV). Tables of numbers are given in Ref. [19]. It is apparent that our data agree very well with the

SLAC data in the range of overlap and exhibit a smooth fall-off with Q^2 .

The double dot-dashed and dot-dashed curves in Fig. 2 represent the RIA calculations of Van Orden, Devine and Gross (VDG) [7] and Hummel and Tjon (HT) [8], respectively. The VDG curve is based on a relativistically covariant calculation that uses the Gross equation [20] and assumes that the virtual photon is absorbed by an off-mass-shell nucleon or a nucleon that is on-mass-shell right before or after the interaction. The HT curve is based on a one-boson-exchange quasipotential approximation of the Bethe-Salpeter equation [21] where the two nucleons are treated symmetrically by putting them equally off their mass-shell with zero relative energy. In both cases the RIA appears to be lower than the data. Both groups have augmented their models by including the $\rho\pi\gamma$ MEC contribution. The magnitude of this contribution depends on the $\rho\pi\gamma$ coupling constant and vertex form factor choices [22]. The VDG model (dashed curve) uses a $\rho\pi\gamma$ form factor from a covariant separable quark model [23]. The HT model (dotted curve) uses a Vector Dominance Model. The difference in the two models is indicative of the size of theoretical uncertainties. Although our data favor the VDG calculations, a complete test of the RIA+MEC framework will require improved and/or extended measurements of the nucleon form factors and of the deuteron $B(Q^2)$, planned at JLab.

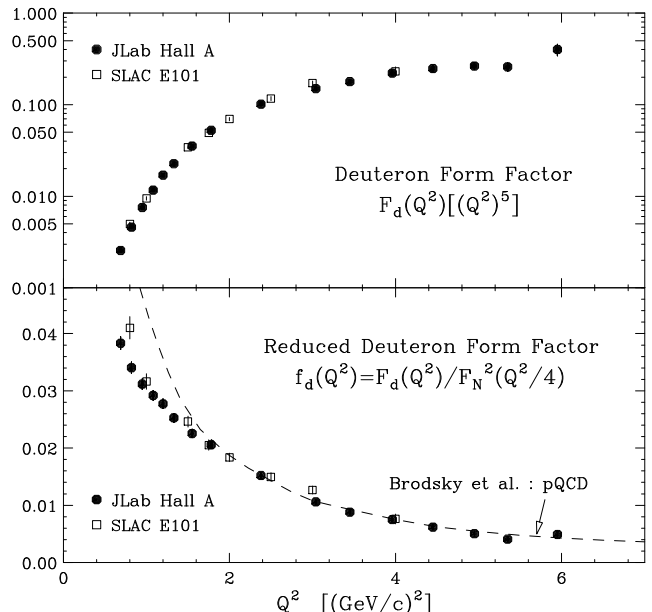


FIG. 4. The deuteron form factor $F_d(Q^2)$ times $(Q^2)^5$ (top) and the reduced deuteron form factor $f_d(Q^2)$ (bottom) from this experiment and from SLAC [4]. The curve is the asymptotic pQCD prediction of Ref. [14] for $\Lambda=100$ MeV, arbitrarily normalized to the data at $Q^2 = 4$ $(\text{GeV}/c)^2$.

Figure 3 shows our data in the “low” Q^2 range where they overlap with data from other laboratories. The previous measurements tend to show two long-standing di-

verging trends, one supported by the SLAC data and the other one by the CEA [3] and Bonn [5] data. Our data agree with the Saclay data [6] and confirm the trend of the SLAC data. It should be noted that another JLab experiment has measured $A(Q^2)$ in the Q^2 range 0.7 to 1.8 (GeV/c)² [24]. The two curves are from a recent non-relativistic IA calculation [25] using the Argonne v_{18} potential without (dot-dashed curve) and with (dashed curve) MEC, and exhibit clearly the necessity of MEC inclusion also in the non-relativistic IA.

Figure 4 (top) shows values for the “deuteron form factor” $F_d(Q^2) \equiv \sqrt{A(Q^2)}$ multiplied by $(Q^2)^5$. It is evident that our data exhibit a behavior consistent with the power law of QDS and pQCD. Figure 4 (bottom) shows values for the “reduced” deuteron form factor [26] $f_d(Q^2) \equiv F_d(Q^2)/F_N^2(Q^2/4)$ where the two powers of the nucleon form factor $F_N(Q^2) = (1 + Q^2/0.71)^{-2}$ remove in a minimal and approximate way the effects of nucleon compositeness [26]. Our $f_d(Q^2)$ data appear to follow, for $Q^2 > 2$ (GeV/c)², the asymptotic Q^2 prediction of pQCD [14]: $f_d(Q^2) \sim [\alpha_s(Q^2)/Q^2][\ln(Q^2/\Lambda^2)]^{-\Gamma}$. Here $\Gamma = -(2C_F/5\beta)$, where $C_F = (n_c^2 - 1)/2n_c$, $\beta = 11 - (2/3)n_f$, with $n_c = 3$ and $n_f = 2$ being the numbers of QCD colors and effective flavors. Although several authors have questioned the validity of QDS and pQCD at the momentum transfers of this experiment [27], [28], similar scaling behavior has been reported in deuteron photodisintegration cross sections at moderate photon energies [29].

In summary, we have measured the elastic structure function $A(Q^2)$ of the deuteron up to large momentum transfers. The results have clarified inconsistencies in previous data sets at low Q^2 . The high luminosity and unique capabilities of the JLab facilities enabled measurements of record low cross sections (the average cross section for $Q^2 = 6$ (GeV/c)² is $\sim 2 \times 10^{-41}$ cm²/sr) that allowed extraction of values of $A(Q^2)$ lower by one order of magnitude than achieved at SLAC. The precision of our data will provide severe constraints on theoretical calculations of the electromagnetic structure of the two-body nuclear system. Calculations based on the relativistic impulse approximation augmented by meson-exchange currents are consistent with the present data. The results are also indicative of a scaling behavior consistent with predictions of dimensional quark scaling and perturbative QCD. Future measurements, at higher Q^2 , of $A(Q^2)$ and $B(Q^2)$ as well as of the form factors of the helium isotopes would be critical for testing the validity of the apparent scaling behavior.

We acknowledge the outstanding support of the staff of the Accelerator and Physics Divisions of JLab that made this experiment possible. We are grateful to the authors of Refs. [7], [8] and [25] for kindly providing their theoretical calculations, and to F. Gross for valuable discussions. This work was supported in part by the U.S. Department of Energy and National Science Foundation, the

Kent State University Research Council, the Italian Institute for Nuclear Research, the French Atomic Energy Commission and National Center of Scientific Research, the Natural Sciences and Engineering Research Council of Canada and the Fund for Scientific Research-Flanders of Belgium.

-
- [1] J. Carlson and R. Schiavilla, *Rev. Mod. Phys.* **70**, 743 (1998); and references therein.
 - [2] C.E. Carlson, J.R. Hiller, R.J. Holt, *Annu. Rev. Nucl. Part. Sci.* **47**, 395 (1997); and references therein.
 - [3] J.E. Elias *et al.*, *Phys. Rev.* **177**, 2075 (1969).
 - [4] R.G. Arnold *et al.*, *Phys. Rev. Lett.* **35**, 776 (1975).
 - [5] R. Cramer *et al.*, *Z. Phys.* **C29**, 513 (1985).
 - [6] S. Platchkov *et al.*, *Nucl. Phys.* **A510**, 740 (1990).
 - [7] J.W. Van Orden, N. Devine and F. Gross, *Phys. Rev. Lett.* **75**, 4369 (1995); and references therein.
 - [8] E. Hummel and J.A. Tjon, *Phys. Rev. Lett.* **63**, 1788 (1989); *Phys. Rev.* **C42**, 423 (1990).
 - [9] P.L. Chung *et al.*, *Phys. Rev.* **C37**, 2000 (1988).
 - [10] J. Carbonell *et al.*, *Phys. Rep.* **300**, 215 (1998).
 - [11] R. Dymarz and F.C. Khanna, *Nucl. Phys.* **A516**, 549 (199); and references therein.
 - [12] T-S. Cheng and L.S. Kisslinger, *Phys. Rev.* **35**, 1432 (1987); H. Dijk and B.L.G. Bakker, *Nucl. Phys.* **A494**, 438 (1989).
 - [13] S.J. Brodsky and G.R. Farrar, *Phys. Rev. Lett.* **31**, 1153 (1973); V.A. Matveev, R.M. Muradyan and A.N. Tavkhelidze, *Lett. Nuovo Cimento* **7**, 719 (1973).
 - [14] S.J. Brodsky, C-R. Ji and G.P. Lepage, *Phys. Rev. Lett.* **51**, 83 (1983).
 - [15] K.B. Unser, CERN report CERN-SL-91-42-BI (1991).
 - [16] R.G. Arnold *et al.*, *Phys. Rev. Lett.* **58**, 1723 (1987); P.E. Bosted *et al.*, *Phys. Rev.* **C42**, 38 (1990); and references therein.
 - [17] P.E. Bosted, *Phys. Rev.* **C51**, 409 (1995).
 - [18] A.T. Katramatou *et al.*, *Nucl. Instr. Meth.* **A267**, 448 (1988); A.T. Katramatou, SLAC report SLAC-NPAS-TN-86-08 (1986).
 - [19] World Wide Web Page of Jefferson Laboratory Hall A: <http://www.jlab.org/Hall-A/publications/papers.html>.
 - [20] F. Gross, *Phys. Rev.* **186**, 1448 (1969); *Phys. Rev.* **D10**, 223 (1974); *Phys. Rev.* **C26**, 2203 (1982).
 - [21] E.E. Salpeter and H.A. Bethe, *Phys. Rev.* **84**, 1232 (1951).
 - [22] H. Ito and F. Gross, *Phys. Rev. Lett.* **71**, 2555 (1993).
 - [23] K.L. Mitchell, Ph.D. Dissertation, Kent State University, 1995; P.C. Tandy, *Prog. Part. Nucl. Phys.* **36**, 97 (1996).
 - [24] D. Abbott *et al.*, submitted to *Phys. Rev. Lett.*
 - [25] R.B. Wiringa, V.G.J. Stoks and R. Schiavilla, *Phys. Rev.* **C51**, 38 (1995); R. Schiavilla and D.O. Riska, *Phys. Rev.* **C43**, 437 (1991).
 - [26] S.J. Brodsky and B.T. Chertok, *Phys. Rev. Lett.* **37**, 269 (1976); *Phys. Rev.* **D14**, 3003 (1976).
 - [27] N. Isgur and C.H. Llewellyn Smith, *Phys. Rev. Lett.* **52**, 1080 (1984); *Phys. Lett.* **B217**, 535 (1989).
 - [28] G.R. Farrar, K. Huleihel and H. Zhang, *Phys. Rev. Lett.* **74**, 650 (1995).
 - [29] C. Bochna *et al.*, submitted to *Phys. Rev. Lett.*